Application of Punctured Turbo Codes with Unequal Error Protection to Wireless ATM Networks

著者	SUN Zhenqiang, KIMURA Shigetomo, EBIHARA Yoshihiko
journal or publication title	IEICE transactions on communications
volume	E84.B
number	5
page range	1319-1327
year	2001-05
権利	電子情報通信学会 本文データは学協会の許諾に基づきCiNiiから複製したものである
URL	http://hdl.handle.net/2241/116928

IEICE TRANS. COMMUN., VOL.E84–B, NO.5 MAY 2001

PAPER

Application of Punctured Turbo Codes with Unequal Error Protection to Wireless ATM Networks

Zhenqiang SUN[†], **Shigetomo KIMURA**[††], *and* **Yoshihiko EBIHARA**[††], *Regular Members*

SUMMARY In the wireless asynchronous transfer mode (ATM) networks, a custom data link control (DLC) layer protocol with stronger error correction ability is needed for mitigating the affect of radio channel errors. This paper applies punctured turbo code schemes to the protection of the header and various payloads in wireless ATM cell, which are realized by the combination of programmable interleaving and puncturing. Their performance is analyzed for Rayleigh fading channel, which shows more significant reduction in cell loss rate (CLR) than the previous systems. Our proposal also provides good balance designs for CLR and the payload bit error rate (BER), and offers potential for future evolutionary improvement of the wireless ATM coding scheme.

key words: *wireless ATM, forward error correction, turbo codes, Rayleigh fading channel, unequal error protection*

1. Introduction

With ATM technology playing an increasing important role in the future broadband networks, it is natural to expect the wireless ATM networks supporting various multimedia services in a seamless manner. But the ATM protocol was designed assuming highly reliable links and point-to-point transmission, which clearly contrasts with the characteristics of the wireless link (high error rates and broadcast transmission). In order to overcome these incompatibilities, the specific protocol layers–medium access control (MAC), data link control (DLC) and wireless network control are incorporated into a mobility-enhanced ATM protocol stack, as illustrated in Fig. 1 [1]. In virtue of the design philosophy of not modifying existing systems unless required, the wireless ATM protocol stack modules are added into the radio module (RM) and base station (BS). For mobility, the mobile ATM protocol stacks are also inserted into the RM, the BS and the standard ATM Switch. The wireless interface of ATM networks is a band-limited channel with multi-path fading and strong interference. Because it has a much stronger error prone characteristics than the wired one, optimal forward error correction (FEC) is needed [2].

FEC system corrects errors by using redundancy bits. Therefore, when its quality increases, its transmission capacity decreases. A tradeoff between quality (coding gain) and capacity (coding rate) is very important in designing FEC systems. In multimedia wireless ATM cell, the importance of the header far outweighs than that of the various payloads. On the other hand, each service requires various payloads with different bit error rate (BER) and delay. So, channel coding is desired to provide different levels of error protection matching to the different sensitivity of source encoded symbols. In order to realize this, one scheme having two different FEC codes for the header and payload is proposed [3], which is applied to the AWA system [4]. In other systems, the variable-rate FEC method controlled by media is proposed to increase total utilization efficiency in multimedia systems [5]. These schemes have unequal error protection (UEP) property that is essential when different portions of the source data do not contribute evenly to overall quality of the decoded information. The UEP is generally achieved at no extra cost in energy, rate, or complexity by multiplexed block or convolutional codes [6].

Turbo codes [7] offer unprecedented coding gains with relatively simple soft iterative decoding. They can also vary the coding rate to offer different error protection levels by using the same component code, available interleaver and different puncturing matrix [8]. From this fact, we have applied two UEP level turbo codes to wireless ATM by changing the rate of turbo codes in [9], and obtained reduction in the cell loss rate (CLR) than the ordinary ATM protection. This paper reviews our proposal and gives the new results in CLR comparing with the previous systems. The relationship between BER and bit position, and the error correction characteristics for each system are also analyzed.

The construction of this paper is in below. Section 2 reviews the wireless ATM cell. Section 3 describes how turbo codes are used to achieve two unequal error protection levels. Performance analysis about CLR and BER are put forward in Sect. 4. Section 5 concludes this paper.

2. Wireless ATM Cell

According to the protocol reference model of broadband integrated service digital networks, ATM cell header error control (HEC) is a physical layer function. The

Manuscript received February 7, 2000.
Manuscript revised September 20, 2000.

[†]The author is a graduate in the Doctoral Program in Engineering, University of Tsukuba, Tsukuba-shi, 305-8573 Japan.
[††]The authors are with the Faculty of the Institute of Information Sciences and Electronics, University of Tsukuba, Tsukuba-shi, 305-8573 Japan.

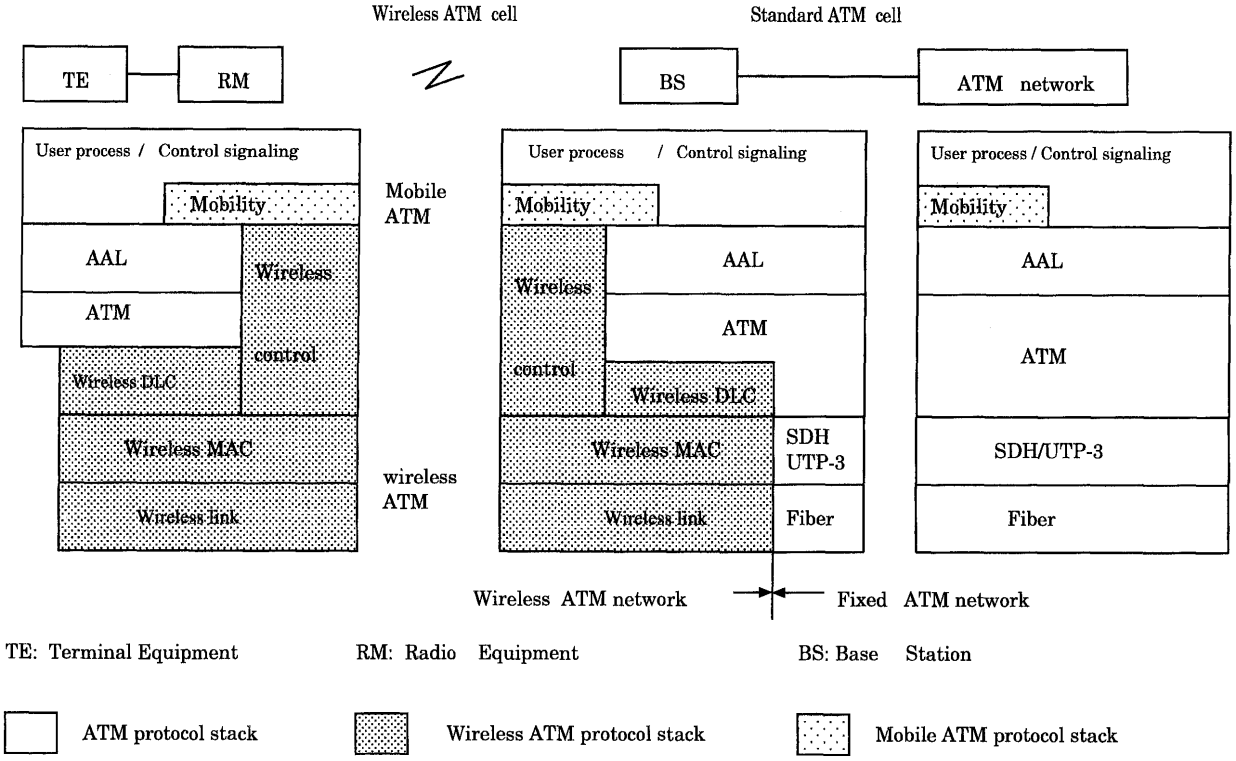

Fig. 1 Wireless ATM protocol stack overview.

HEC is a single-bit error correction and multiple-bit error detection cyclic redundancy code (CRC), and only employed in the ATM cell header but not in the cell payload in order to avoid incorrect forwarding due to header error. HEC code controls 8 redundant bits out of 40 bits in a cell header.

But in the wireless ATM network, the above HEC alone is not sufficient. For mitigating the effect of radio channel errors before cells are released to the ATM network layer, the wireless ATM needs a new DLC layer protocol. In wireless ATM, cells arrive into the DLC layer corresponding to the particular virtual circuit (VC). For the smaller number of users and the scarcity of bandwidth in wireless networks, the relatively large addressing overhead of ATM being designed for large wire-line networks must be avoided. Therefore, the format of wireless ATM cell is proposed as shown in Fig. 2 [6]. Since wireless communication systems have high error rates in general, CLR may be improved by reducing the packet length [1]. In addition, depending on the achievable channel speed, the type of low-speed applications (e.g., 8 kb/s voice CODEC, e-mail message, etc) to be supported, and the relative importance of high wireless channel efficiency, it may be necessary to compromise on this requirement and use wireless data-link packets with payloads that are integer submultiples of an ATM cell, i.e., $\frac{48}{m}$, such as 16 ($m = 3$) or 24 ($m = 2$) bytes [2]. After compressing essential ATM header information, only two bytes are assigned for VC identifier (VCI) and control information in the wireless ATM header. Besides, this DLC

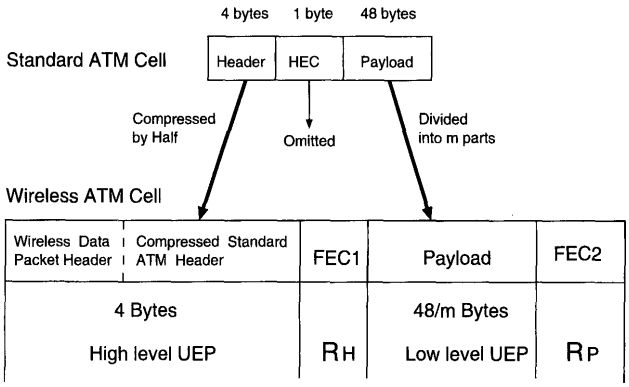

Fig. 2 DLC packet format of wireless ATM cell (using two coding rate FEC).

layer should contain error control, service type definition, segmentation and reassembly and handoff indicator. From this fact, we introduce another 2 bytes for these information in the wireless ATM header, called the wireless data packet header.

This paper only discuss the FEC schemes of DLC protocol for stream mode services. Based on this schemes, the hybrid automatic repeat request (ARQ) schemes can be constructed for the packet mode services. In FEC schemes, header bits in ATM cell are considered to be more important than payload bits. In order to ensure correct delivery and low loss rate, a turbo code scheme (FEC1) with low local coding rate R_1 can be used for a header. At the same time, the turbo code for the payload (FEC2) is designed to be

with higher rate R_2 than the one of FEC1 for effective transmission. Therefore, the HEC in the standard ATM header is replaced by FEC1 and FEC2.

3. Two Rate Turbo Code Scheme for Wireless ATM

3.1 Description of Turbo Encoder

Turbo code is a novel class of parallel concatenated recursive systematic code, which includes interleaver, puncturer and some component encoders. Let $G_c = [I_N|G_0]$ be systematic generator matrix for two same component encoders of rate $1/n$ by trellis termination at all [7], where I_N is $N \times N$ identity matrix, G_0 is $N \times r_0$ parity check part of G_c, and r_0 is the length of redundancy vector. In order to achieve the best results, component codes should be recursive systematic codes (RSC) with primitive feedback polynomials. An interleaver of length N is described by a $N \times N$ permutation matrix $\prod$, which contains a single "1" in each row and column. The type and size of interleaver influence the performance of turbo codes to a great extent. Generally, there is a puncturer in the output of encoder to obtain a desired rate by puncturing appropriate encode bits.

Because the best performance is obtained when encoded bits at the systematic positions of encoded bits are not punctured [7], an puncturing matrix P takes the block-diagonal form of $[I_N|P_0|P_0]$, where P_0 is the puncturing matrix of size $r_0 \times r_1$ (r_1 is the length of a redundancy vector after being punctured). Then, the generator matrix of the turbo code is:

$$G = \left[I_N|G_0|\prod G_0\right] P = \left[I_N|G_0P_0|\prod G_0P_0\right]. \quad (1)$$

The rate of turbo code G is:

$$R = \frac{N-t}{2r_1+N} = \frac{N-t}{2w(P_0)+N}. \quad (2)$$

Here, $w(.)$ denotes the Hamming weight. t is the number of symbols needed for the trellis termination, in general, which is equal to the memory of the component encoder.

If the same component encoders have a rate of $\frac{1}{n}$, the turbo encoder outputs $2n-1$ symbols for each input symbol when puncturing is not used. After puncturing, the encoding rate (local rate) R becomes:

$$\frac{1}{2n-1} \le R \le 1. \quad (3)$$

It is worth noting that the performance of turbo codes largely depends on their input block length. The BER becomes lower as their input block length becomes larger. But the turbo codes with short block length like N=420 and 100 bits can still achieve much lower BER [11], [14].

3.2 The Realization of Punctured Turbo Codes with UEP

In order to provide UEP, the different local rates are obtained by puncturing output of the same basic low rate turbo code. Generally, the redundancy symbols corresponding to low-importance input symbols are punctured with more bits. Through appropriate puncturing of the parity sequences, turbo codes of any rate are attainable. Then, only one encoder and one decoder circuits are needed for various coding rates, since their perforation matrices can be programmable.

For two rate turbo codes, two different punctured matrices are needed. However, UEP cannot be achieved only by puncturing. Available interleaver is needed to provide "support set invariance" property [8] that a permutation can map each support set onto the same set of positions in the interleaved frame.

The $N-t$ encoder input symbols are partitioned into 2 importance classes S_1 (its size is N_1 and local rate is R_1) and S_2 (its size is N_2 and local rate is R_2), ordered in decreasing order of importance, where:

$$N_1 + N_2 = N - t. \quad (4)$$

In this way, we obtain a FEC scheme where each class S_l of input symbols is locally protected by a punctured turbo code of rate R_l (l=1,2). The relationship between overall rate and local rates is:

$$N_1/R_1 + N_2/R_2 = (N-t)/R. \quad (5)$$

According to the specific BER targets, we can endow an UEP turbo code by controlling a set of local rates, or the support set fragmentation into intervals. So, the application of variable punctured turbo code allows bandwidth efficiency to be exchanged for reliability for the same hardware complexity.

3.3 Two Level UEP Scheme for the Wireless ATM Cell

In order to apply the two rate turbo code to the wireless ATM, we portion the encoder input frame of the wireless ATM cell into two importance classes S_1 and S_2 with size $N_1 = 32$ bits (4 bytes) and $N_2 = 384/m$ bits ($48/m$ bytes) corresponding to header and payload [9]. Since t is generally much less than N_1 or N_2, the t symbols can be included in the least important class S_2 with negligible information rate decrease, as shown in Fig. 3. Because the encoder starts and ends in state zero for MAP decoder, the information bits at the beginning and the end of a transmitted block have a lower bit error ratio. Then, the header bits are positioned at the beginning (first 16 bits) and the end (last 16 bits) of the frame, and the payload bits with the trellis termination t (equal to 4 bits when using 16 state component

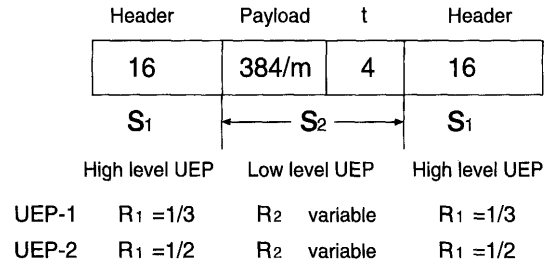

Fig. 3 Encoder input frame for class 1,2.

encoder) are positioned at the middle of the frame. The total bits N of the frame is:

$$N = N_1 + N_2 + t = 32 + \frac{384}{m} + 4 = 36 + \frac{384}{m}.$$

In this paper, we suppose the two level UEP scheme of each wireless ATM cell is not related to the modulation method. Therefore, m can be selected in divisors of the payload length, and there does not exist the problems such as the phase ambiguities.

To support the quality of service (QoS) required by the different types of data, the ATM payload is encoded for varying degrees of error protection according to the required QoS identified in the ATM header. That is to say, for one VC, there is a corresponding FEC1 and FEC2, which is adaptable to the different services. As shown in Fig. 3, we consider the following two schemes with different quality levels. For UEP-1 scheme, we set $R_1 = \frac{1}{3}$ turbo code for the header and various R_2 turbo code for payloads. Its overall coding rate R becomes:

$$R = \frac{N - t}{N_1 \times 3 + \frac{N_2}{R_2}} = \frac{32 + \frac{384}{m}}{96 + \frac{\frac{384}{m}}{R_2}}. \quad (6)$$

For example, $R \doteq \frac{2}{3}$ when m=1 and $R_2 = \frac{3}{4}$, or when m=2 and $R_2 = \frac{5}{6}$.

Its throughput T is equal to:

$$T = \frac{N_2}{N_1 \times 3 + \frac{N_2}{R_2}} = \frac{\frac{384}{m}}{96 + \frac{\frac{384}{m}}{R_2}}. \quad (7)$$

For UEP-2 scheme, $R_1 = \frac{1}{2}$ and various R_2, the overall coding rate R becomes:

$$R = \frac{N - t}{N_1 \times 2 + \frac{N_2}{R_2}} = \frac{32 + \frac{384}{m}}{64 + \frac{\frac{384}{m}}{R_2}}. \quad (8)$$

For example, $R \doteq \frac{3}{4}$ when m=1 and $R_2 = \frac{4}{5}$, or when m=2 and $R_2 = \frac{5}{6}$.

Its throughput T is equal to:

$$T = \frac{N_2}{N_1 \times 2 + \frac{N_2}{R_2}} = \frac{\frac{384}{m}}{64 + \frac{\frac{384}{m}}{R_2}}. \quad (9)$$

Figure 4 and Fig. 6 show the relationships between R and m, R_2 for UEP-1 and UEP-2, respectively. For comparition, we cite the results of the BC and AWA. BC is (49,16) 6 error-correcting block code for header and variable rate for various payload [10]. AWA represents (56,32) 4-bit error correction for header and (208,192) double error correction for payload [3].

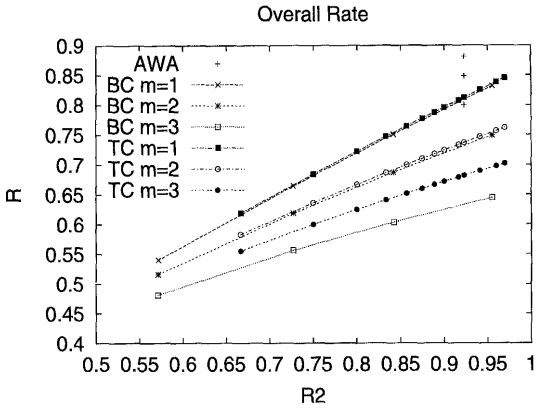

Fig. 4 The value of overall rate for UEP-1.

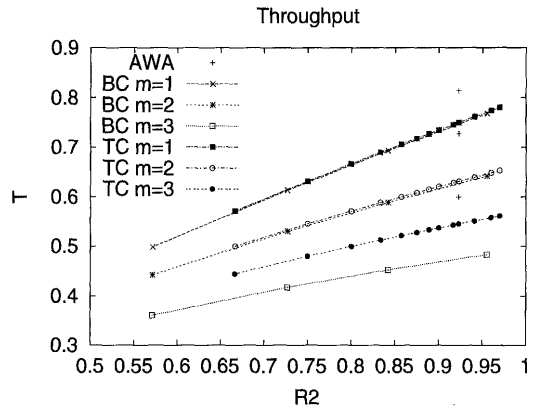

Fig. 5 The value of throughput for UEP-1.

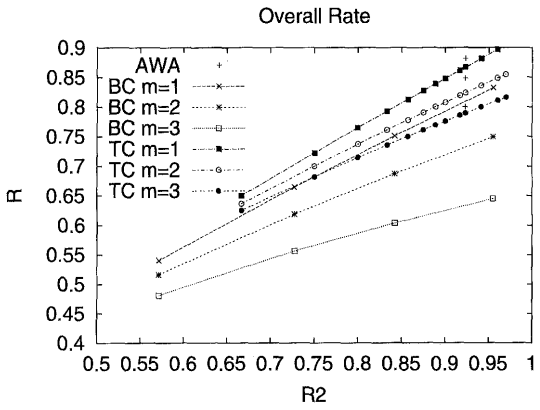

Fig. 6 The value of overall rate for UEP-2.

Since we suppose ARQ is not implemented at the DLC layer, e.g., for stream mode CBR/VBR services, the throughput of DLC strategy is mainly influenced by the overall rate. Figure 5 and Fig. 7 show the relationships between T and m, R_2 for UEP-1 and UEP-2, respectively. Then from these figures, we know UEP-1 scheme can achieve the same throughput as BC, UEP-2 scheme can achieve the throughput as high as AWA

when R_2 become bigger. These figures show that the throughput of UEP-1 and UEP-2 are very lower for $m = 3$. Since the header of the cell degrades the throughput as m increases, the cases $m \geq 3$ are not considered in the rest of paper.

4. Performance Analysis

Figure 8(a) illustrates the adding and removing of HEC/FEC. When the RM receives ATM cell from the TE, one bit error correction and multiple bit error detection are performed. HEC in the cell is replaced by FEC1 and FEC2, and the cell is transmitted to the BS. When errors in the header can not be corrected at the BS, the cell is discarded in the BS. Beside the wireless section in the BS, new HEC of the cell is generated for the wired section.

The Rayleigh fading AWGN channel model represents the worst case model for the design engineer while offering analytical convenience [11]. Furthermore, a coherent demodulation strategy is assumed so as to compensate the effects of fading on signal phase, therefore, we will be concerned only with the amplitude fading. In this case, the part from the sender to the receiver in Fig. 8(a) is expressed as Fig. 8(b), which is the simulation environment to evaluate our proposal scheme, where b_k and $\hat{b_k}$ are the original and the decoded bits, respectively. After b_k is encoded and then modulated, X_k is obtained. Y_k is received data of X_k described as follow:

$$Y_k = a_k X_k + n_k, \tag{10}$$

where the fading amplitude a_k is a real Rayleigh-distributed random variable with $E(a_k^2)$=1 and n_k is the complex white Gaussian noise with one-sided power special density N_0.

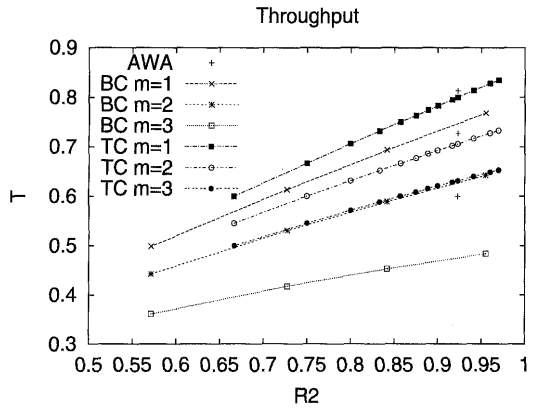

Fig. 7 The value of throughput for UEP-2.

4.1 Bit Error Rate for UEP Turbo Code Scheme

Firstly, we examine the bit error rate of two level UEP schemes for wireless ATM. Our simulations are proceeded for UEP-1 schemes with $m = 1$, $R_2 = \frac{3}{4}$ and $m = 2$, $R_2 = \frac{5}{6}$, UEP-2 schemes with $m = 1$, $R_2 = \frac{4}{5}$, and $m = 2$, $R_2 = \frac{5}{6}$, which can be extended to general case.

For turbo code with $R = \frac{1}{3}$, puncturing is not needed. For turbo codes with $R = \frac{1}{2}, \frac{3}{4}, \frac{4}{5}$, the elementary punctured matrices are selected as follows, in term of generality [15],

$$\begin{bmatrix} 1 & 0 \end{bmatrix}^T,$$

$$\begin{bmatrix} 1 & 0 & 0 & 0 & 0 & 0 \end{bmatrix}^T,$$

$$\begin{bmatrix} 1 & 0 & 0 & 0 & 0 & 0 & 0 & 0 \end{bmatrix}^T.$$

When $N = 420$ bits, and the component encodes are considered as two identical half rate systematic recursive convolutional encoders with generator (31,33),

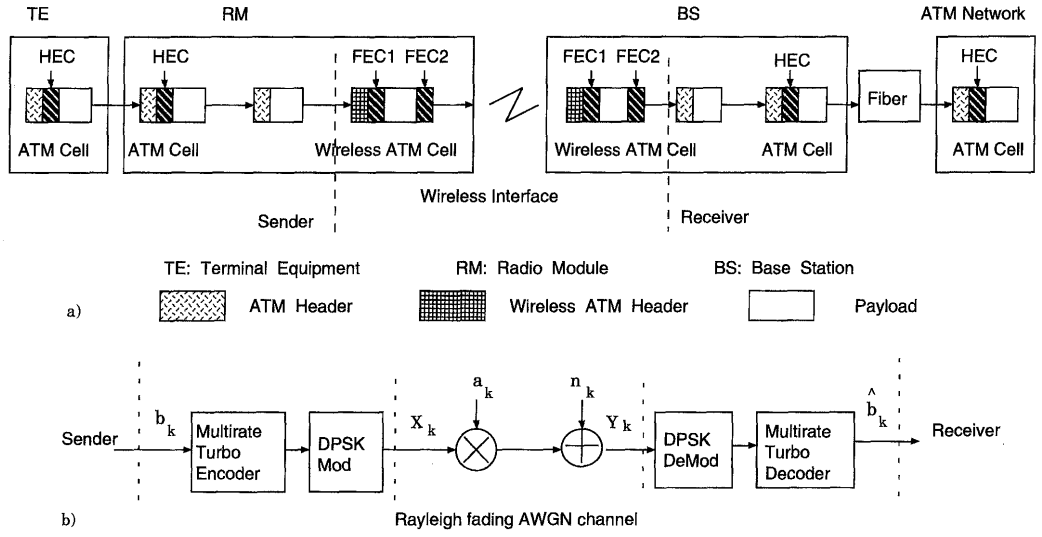

Fig. 8 The realization of two level turbo code scheme in the wireless ATM networks.

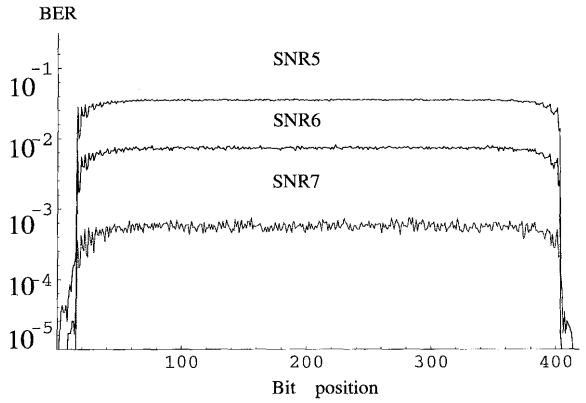

Fig. 9 The relationship between BER of UEP-1 scheme (m=1) and bit position for a Rayleigh fading channel ($R = \frac{2}{3}$).

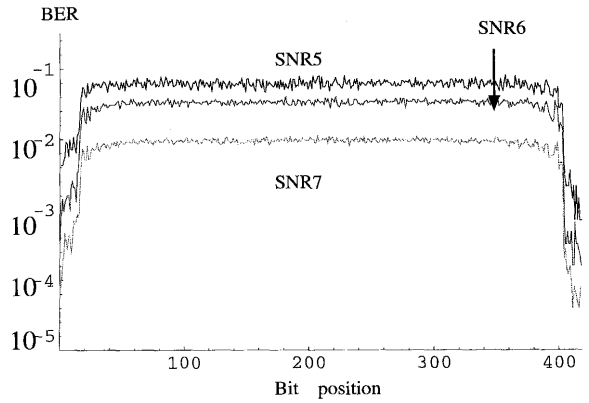

Fig. 11 The relationship between BER of UEP-2 scheme (m=1) and bit position for a Rayleigh fading channel ($R = \frac{3}{4}$).

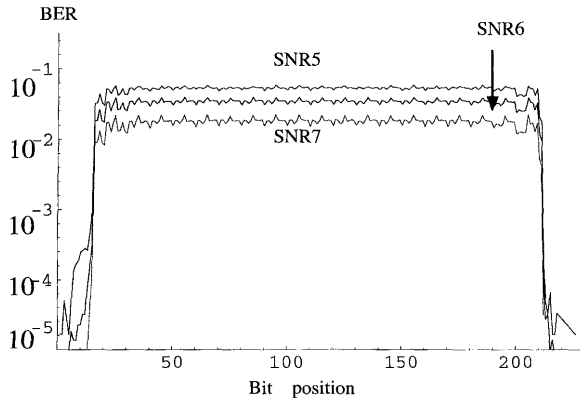

Fig. 10 The relationship between BER of UEP-1 scheme (m=2) and bit position for a Rayleigh fading channel ($R = \frac{2}{3}$).

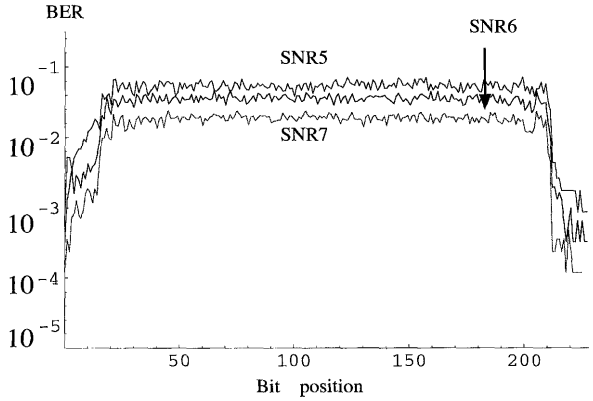

Fig. 12 The relationship between BER of UEP-2 scheme (m=2) and bit position for a Rayleigh fading channel ($R = \frac{3}{4}$).

$K = 5$. Decoding is implemented by the iterative decoder as described in [7]. A minimum of 1000 bit errors is counted for each simulated point. Here, we use a simple way to simulate puncturing, which is to set the received parity samples corresponding to the punctured parity bits to zero in the computation of LAPP (log a posteriori probability) ratio. Thus, puncturing need not be performed at the encoder.

The BERs of the UEP-1 and the UEP-2 for a Rayleigh fading channel as a function of bit position for a block 420 bits ($m = 1$) and 228 bits ($m = 2$) are plotted in Figs. 9 to 12. Where SNR5, SNR6 and SNR7 represent the cases of E_s/N_0 =5,6,7 dB, respectively. These realize two level UEP with two level interleaving and puncturing. It is shown that the performance of the turbo code degrades significantly if puncturing is employed. But there is no "spill over" effect when switching from one rate to another. The expected error probability can be achieved by changing rate.

These figures show that the BER performance when $m = 1$ is better than the one when $m = 2$. Therefore $m = 1$ should be selected for higher throughput and lower BER. In the rest of paper, m is always fixed to 1.

4.2 Cell Loss Rate Bound Using Turbo Code

One of the most important performance parameters in ATM cell transport is CLR, which is defined by the ratio of the total numbers of lost cells to the total numbers of transmitted cells. When an ATM cell is sent over a wireless interface, there are three possible outcomes:

1. The cell is accepted by the intended mobile.
2. The cell is accepted by the wrong mobile.
3. The cell is not accepted by any mobile.

It is assumed that the probability of the second outcome is negligibly small. In addition there is a negligibly small probability that a cell accepted by the intended mobile will contain incorrect embedded QoS information. As a result, a header is either decoded correctly or the cell is lost [10]. For CBR and rt-VBR, when a header portion contains errors that can not be corrected, the cell is generally misdirected and regarded as lost cell outcome [12].

Idealizing to the case of perfect interleaving, the channel is considered memoryless, that is, the fading process is independent from bit to bit. The average probability of bit error for binary phase shift keying

signal over a Rayleigh fading channel is given by [13]:

$$P_b = \frac{1}{2}\left(1 - \sqrt{\frac{RE_b/N_0}{1+RE_b/N_0}}\right) \tag{11}$$

where E_b/N_0 is the average signal-to-noise ratio (SNR) per bit. For an uncoded header (4 bytes), the probability of cell loss is given by:

$$P_{uncoded} = 1 - (1-P_b)^{32}. \tag{12}$$

For HEC, there are two operating modes: the correction mode and the detection mode. In the correction mode, a single-bit error can be corrected and cells with multiple-bit errors are discarded. Its probability is: $P_{cor.} = P_0$, where the probability of no error in one cell header $P_0 = (1-P_b)^{40}$. In the detection mode, all cells with detected errors in header are discarded, which probability is: $P_{det.} = 1 - P_0$. Besides, the probability of single-bit error in one cell header $P_1 = 40P_b(1-P_b)^{39}$ and the probability of multiple-bit errors in one cell header $P_2 = 1 - P_0 - P_1$. Then, the probability of cell loss is:

$$\begin{aligned} P_{HEC} &= P_{det.}(P_1+P_2) + P_{cor.}P_2 \\ &= (1-P_0)(1-P_0) + P_0(1-P_0-P_1) \end{aligned} \tag{13}$$

If the (n,k) t-bit error correcting block code is applied to the header of wireless ATM cell, the probability of cell loss is given by:

$$P_{block} = \sum_{i=t+1}^{n} {}_nC_i(1-P_b)^{n-i}P_b^i. \tag{14}$$

If an $(nl-m,l)$ punctured convolutional code (PCC) with the minimum free Hamming distance d_f is applied to a header, the probability of cell loss for coded systems is given by:

$$P_C = 1 - (1-P_{cc})^{32}, \tag{15}$$

where P_{cc} is the bit error probability of wireless ATM header after using PCC. With Viterbi decoding, P_{cc} is upper bounded by [13]:

$$P_{cc} \le \frac{1}{l}\sum_{d=d_f}^{\infty} c_d P_d, \tag{16}$$

where c_d is the total number of error bits produced by the incorrect paths, which depends on the code, and P_d is the probability that the wrong path at distance d is selected, which depends on the channel properties.

When using soft decisions and full channel state information (CSI), P_d can be upper bounded by [13]:

$$P_d \le \frac{1}{2}\left(\frac{1}{1+RE_b/N_0}\right)^d. \tag{17}$$

In case of hard decision, P_d is given by [13]:

$$P_d = \begin{cases} \displaystyle\sum_{i=\frac{d+1}{2}}^{d} {}_dC_i(1-P_b)^{d-i}P_b^i, & \text{for } d \text{ is odd} \\ P_{d-1}, & \text{for } d \text{ is even} \end{cases} \tag{18}$$

If the $R = \frac{1}{3}$ turbo code is applied to a header, the probability of cell loss for coded systems is given by:

$$P_T = 1 - (1-P_{tc})^{32}, \tag{19}$$

where P_{tc} is the bit error probability of a wireless ATM header after using turbo code. Assuming a uniform interleaver and concerning the weight distribution of the codewords as [14], P_{tc} can be upper bounded by:

$$P_{tc} \le \sum_{i=1}^{N}\left(\frac{i}{N}\right) {}_NC_i E_{d/i}[P_2(d)], \tag{20}$$

where $E_{d/i}[.]$ is an expectation with respect to the distribution $p(d/i)$. $p(d/i)$ is the probability that an interleaving scheme maps an input weight i to produce a codeword with total weight d. $P_2(d)$ is the probability of choosing a specific wrong codeword differing from the correct codeword in d bit positions. For a full-interleaved Rayleigh fading channel with CSI, it can be upper bounded by [11]:

$$P_2(d) \le \frac{1}{2}\left[1 - \sqrt{\frac{RE_b/N_0}{1+RE_b/N_0}}\right]\left[\frac{1}{1+RE_b/N_0}\right]^{d-1}. \tag{21}$$

For a full-interleaved Rayleigh fading channel without CSI, it can be upper bounded by [11]:

$$P_2(d) \le \left[e^{\frac{\gamma}{\beta}}\frac{\sqrt{1+\frac{2}{\beta}}-1}{\sqrt{1+\frac{2}{\beta}}+1}\right]^d, \tag{22}$$

where $\beta = \sqrt{\gamma^2-1}$ and $\gamma = RE_b/N_0$.

Figure 13 shows the CLR versus SNR analytic upper bound over a fully interleaved Rayleigh fading channel when m=1. In this figure, TC-SI and TC-NSI are $R = \frac{1}{3}$ equal error protection (EEP) turbo codes decoding with and without CSI, respectively. HCC and SCC represent the results of $R = \frac{1}{3}$ convolutional code using hard and soft decisions, respectively. BC is (49,16) 6 error-correcting block code for header [10], whose rate is equal to $\frac{16}{49} \doteq \frac{1}{3}$, about the same as the turbo code. AWA curve represents (56,32) 4-bit error correction for header [3], whose rate is equal to $\frac{32}{56} = \frac{4}{7} > \frac{1}{3}$. Though the rate for header in AWA is larger than the one in turbo code, the overall rates of both codes are about the same. HEC curve represents the HEC only for the header. This shows that the SNR gains are still remarkably high for short frames (N=420 bits). Therefore the turbo codes greatly decreases the degree of cell loss in theory. For example, Fig. 13 indicates that the

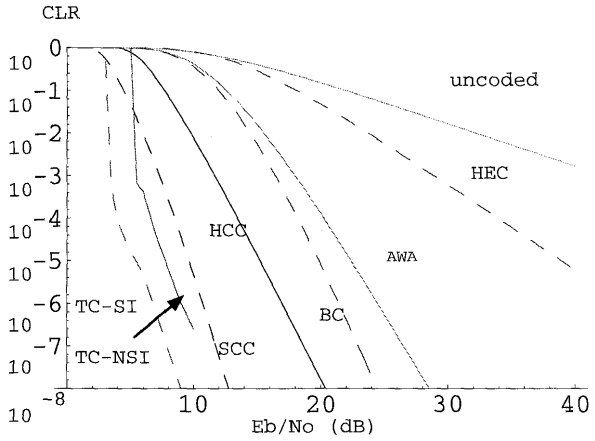

Fig. 13 The CLR versus E_b/N_0 analytic upper bound over fully interleaved Rayleigh fading channel (having about the same overall rate R and m=1).

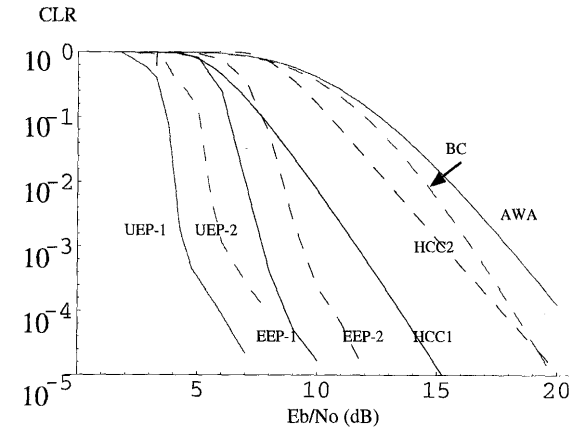

Fig. 14 The CLR versus E_b/N_0 for the UEP and the EEP turbo codes (having about the same overall rate R and m=1) over fully interleaved Rayleigh fading channel without CSI.

$R = \frac{1}{3}$ turbo code using BCJR-MAP decoding with CSI realizes 30 dB gain over the HEC system, 16 dB gain over the AWA scheme, 14 dB gain over the (49,16) block code, 9 dB gain over the $R = \frac{1}{3}$ convolutional code with hard decision and 5 dB gain over the $R = \frac{1}{3}$ convolutional code with soft decision at CLR of 10^{-4}.

For the low SNR region, due to the divergence of union bound, analysis evaluation of the turbo codes is too difficult to be proven. Therefore, we must examine their performance based on simulation in the next subsection.

4.3 Cell Loss Rate for UEP Turbo Code Scheme

In our simulation, wireless headers are treated separately from payloads, i.e., cells with errors at their headers are discarded but those with errors in the payload are not, which is in line with the basic ATM philosophy [10].

In Fig. 14, the UEP turbo code is compared with the EEP turbo code with the same overall frame length

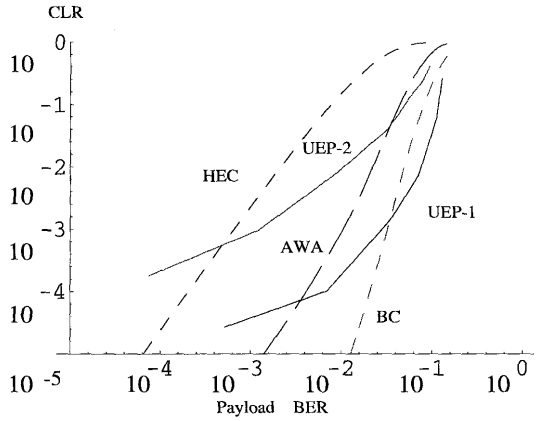

Fig. 15 Error correction characteristics for UEP-1 and UEP-2 (m=1).

$N = 420$ bits and about the same overall rate. UEP-1 have the total rate $R \doteq 0.678$, about the same as the coding rate $R = \frac{2}{3}$ of EEP-1. UEP-2 have the total rate $R \doteq 0.758$, about the same as the coding rate $R = \frac{3}{4}$ of EEP-2. This figure shows the CLR versus E_b/N_0 for the UEP and the EEP turbo codes over a full-interleaved Rayleigh fading channel without CSI. In order to make the comparison between UEP and EEP turbo code independent from iterative decoding, the larger number of iterations, i.e., 20 is chosen. EEP is with a general random interleaver and uniform nonrandom puncturing [16]. Suppose CLR $\leq 10^{-3}$ (i.e. PCS applications) is required, UEP-1 without CSI needs $E_b/N_0 = 4.4$ dB, while EEP-1 without CSI needs $E_b/N_0 = 7.6$ dB. So, the coding gain of UEP-1 scheme with respect to EEP-1 scheme is 3.2 dB. Besides, AWA and BC are the same as Fig. 9. HCC1 and HCC2 represent the results of $R = \frac{1}{3}$ and $R = \frac{1}{2}$ convolutional codes for header, respectively. Obviously, they are worse than the turbo codes with about the same overall rate.

4.4 The Balance between Header CLR and Various Payload BER

It is extremely efficient from the viewpoints of coding gain and coding rate when the same balanced design for CLR and the payload BER is created as the HEC for a wired ATM [3]. The relationship between CLR and the payload BER over fully interleaved Rayleigh fading channel is shown in Fig. 15, where three dashed lines represent BC, AWA and HEC, and two solid lines are UEP-1 and UEP-2, respectively. BC denotes (49,16) 6 error-correcting block code for header and (402,384) 2 bit error correcting block code for payload. Obviously, UEP-1 and UEP-2 schemes have better balance performance than BC and AWA, respectively.

5. Conclusions

In this paper, the two rate turbo code scheme is ap-

plied to realize two protection levels, which is considered to be suitable for the wireless ATM. The wireless ATM cell header is protected by a relatively powerful turbo code to ensure correct delivery and low cell loss. The payload is protected by relatively high transmission turbo code having lower coding gains. A whole family of turbo codes with different rates is available by using the same encoder and the same iterative decoder, though the puncturing rule and interleaver are only needed to change. From the analysis of CLR and BER for several coding rates, we obtain that the applications of punctured turbo codes result in a significant decrease in CLR relative to that of the other famous FEC schemes. This is accomplished with a minimal increase in bandwidth. Besides, the performance results show that our schemes have a good balance design between CLR and payload BER, too.

In order to be able to apply to the stream mode services, we utilize the small interleaver size (N=420 bits) for smaller delay. For the packet services with properties of smaller CLR and allowable delay, the larger interleaver size (e.g. the multiples of 420 bits) should be available. In addition, the hybrid ARQ can be realized on a basis of this FEC schemes.

References

[1] M. Umehira, H. Matsue, and T. Murase, "Development of a prototype ATM wireless access system for nomadic multimedia services," NTT Reviews, vol.10, no.5, pp.88–97, Sept. 1998.
[2] D. Raychaudhuri and N.D. Wilson, "ATM-based transport architecture for multiservices wireless personal communication networks," IEEE J. Sel. Areas Commun., vol.12, no.8, pp.1401–1414, Oct. 1994.
[3] S. Aikawa, Y. Motoyama, and M. Umehira, "Forward error correction schemes for wireless ATM," Proc. ICC'96, pp.454–458, June 1996.
[4] S. Aikawa, Y. Nakayama, S. Kurosaki, and M. Hiraki, "TDMA and antenna control technologies for ATM wireless access prototype," NTT Reviews, vol.10, no.5, pp.113–119, Sept. 1998.
[5] S. Aikawa, H. Sato, and T. Yoshida, "Performance analysis of variable-rate FEC for multimedia radio communications," IEICE Trans. Commun., vol.E77-B, no.9, pp.1104–1113, Sept. 1994.
[6] Z. Sun, S. Kimura, and Y. Ebihara, "Adaptive two-level unequal error protection convolutional code scheme for wireless ATM networks," Proc. IEEE INFOCOM'2000, pp.1693–1697, March 2000.
[7] C. Berrou, A. Glavieux, and P. Thitimajshima, "Near Shannon limit error-correcting codes," Proc. ICC'93, pp.1064–1070, May 1993.
[8] G. Caire and E. Biglieri, "Parallel concatenated codes with unequal error protection," IEEE Trans. Commun., vol.46, no.5, pp.565–567, May 1998.
[9] Z. Sun, S. Kimura, and Y. Ebihara, "Two protection level turbo code scheme for wireless ATM," Proc. ICOIN-14, 2A1, Jan. 2000.
[10] D. Moore and M. Rice, "Variable rate error control for wireless ATM networks," Proc. ICC'95, pp.988–992, June 1995.
[11] E.K. Hall and S.G. Wilson, "Design and performance analysis of turbo codes on Rayleigh fading channels," Proc. 5th Mini-conference on Communications, GLOBECOM'96, Nov. 1996.
[12] A. Ohta, T. Sugiyama, F. Nuno, M. Yoshioka, A. Jozuka, and Y. Sagawa, "Technologies for ATM interface of prototype ATM wireless access equipment," NTT Reviews, vol.10, no.5, pp.120–126, Sept. 1998.
[13] J.G. Proakis, Digital communications, 3rd ed., McGraw-Hill, 1995
[14] S. Benedetto and G. Montorsi, "Unveiling turbo codes: Some results on parallel concatenated coding schemes," IEEE Trans. Inf. Theory, vol.44, no.2, pp.409–421, March 1996.
[15] M.G. Kim, "On systematic punctured convolutional codes," IEEE Trans. Commun., vol.45, no.2, pp.133–139, Feb. 1997.
[16] C. Berrou and A. Glavieux, "Near optimum error correcting coding and decoding: Turbo coding," IEEE Trans. Commun., vol.44, no.10, pp.1261–1271, Oct. 1996.

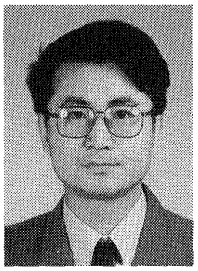

Zhenqiang Sun is a graduate in the Doctoral Program in Engineering, University of Tsukuba, Tsukuba-shi, Japan. He received his B.E. and M.E. degrees in Nanjing Posts and Telecommunications University, People's Republic of China in 1984 and 1987, respectively. His research interests are in forward error correcting code, wireless ATM, and signaling system of communication networks.

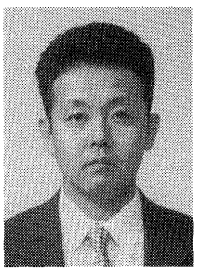

Shigetomo Kimura was born in 1967. He received the D.Info. degree in information science from Tohoku University in 1995. He is currently a Lecturer of Institute of Information Sciences and Electronics, the University of Tsukuba since 1995. His primary research interests are in the areas of algebraic formulation of concurrent processes and program synthesis by inductive inference. He is a member of IPSJ, JSSS, ACM and IEEE.

Yoshihiko Ebihara was born in 1947. He received the B.E., M.E., and D.E. degrees in electrical communication engineering all from Tohoku University, in 1970, 1972, and 1978, respectively. From 1973 to 1975, he was on a staff of ALOHA system project in the University of Hawaii. In 1975 he was appointed a research assistant in Institute of Electrical Communication, Tohoku University. He was appointed a lecturer and a Associate Professor at Institute of Information Sciences and Electronics the University of Tsukuba, in 1976 and 1985 respectively. From 1998, he presided over the Science Information Processing Center of the University of Tsukuba as a director. He is currently a professor of Institute of Information Sciences and Electronics, the University of Tsukuba, since 1993 and he is a chair of the Institute from 2000. His primary research interests include computer network, performance measurement distributed data base management and digital communication system. He is a member of IPSJ.